



Abundance gradients to trace galaxy formation and evolution: the Galactic disk

B. Lemasle¹, G. Bono^{2,3}, V. D'Orazi^{4,5}, M. Franchini⁶, and H. Jönsson⁷

¹ Astronomisches Rechen-Institut, Zentrum für Astronomie der Universität Heidelberg, Mönchhofstr. 12-14, 69120 Heidelberg, Germany

² Dipartimento di Fisica, Università di Roma Tor Vergata, via della Ricerca Scientifica 1, 00133 Rome, Italy

³ INAF - Osservatorio Astronomico di Roma, via Frascati 33, Monte Porzio Catone, Rome, Italy

⁴ INAF - Osservatorio Astronomico di Padova, vicolo dell'Osservatorio 5, I-35122 Padova, Italy

⁵ School of Physics and Astronomy, Monash University, Clayton, VIC 3800 Melbourne, Australia

⁶ INAF - Osservatorio Astronomico di Trieste, Via G. B. Tiepolo 11, Trieste, I-34143, Italy

⁷ Materials Science and Applied Mathematics, Malmö University, SE-205 06 Malmö, Sweden

Received: 5 September 2022; Accepted: 4 October 2022

Abstract.

Abundance gradients are one of the few observables constraining the chemo-dynamical models of the Milky Way disk. Here, we review recent improvements regarding the determination of chemical abundances of young stellar systems, Cepheids, and RGB stars, that are used to trace abundance gradients, before focusing on the oxygen gradient.

Key words. Stars: abundances – Stars: atmospheres – Stars: Population II – Galaxy: globular clusters – Galaxy: abundances – Cosmology: observations

1. Introduction

Chemo-dynamical evolution models usually assume an inside-out scenario (Matteucci & Francois 1989), where the formation timescale of the thin disk increases with radius. Given the complicated interplay between radial mixing of gas, radial migration of stars, the infall rate, the star formation rate, the presence (or not) of a gas density threshold to allow for star formation, etc; and the different manners these physical processes are implemented, models provide different outcomes. The time evolution of gra-

dients enables us to discriminate models predicting a steepening of the gradients with time from those predicting a flattening (Tosi 1996).

For a long time, abundance gradients were relying on a few tracers: H II regions (e.g., Vilchez & Esteban 1996), O/B-type stars (e.g., Daflon & Cunha 2004), open clusters (e.g., Friel et al. 2002), Cepheids (e.g., Harris 1981), planetary nebulae (e.g., Costa et al. 2004), because their classification is straightforward and their distances are known, although with different levels of accuracy. They cover different age

ranges, allowing us to trace the entire chemical evolution of the thin disk. However, the number of elements available and the accuracy of the chemical abundances vary from tracer to tracer. Gaia astrometry (Gaia Collaboration et al. 2016) enabled the use of Red Giant Branch (RGB) stars by providing accurate distances, while also improving (directly or indirectly) the distances of other tracers.

In this paper, we review chemical abundances and abundance gradients derived from young stellar systems (Sect. 2), Cepheids (Sect. 3), and RGB stars (Sect. 4). In Sect. 5, we focus on the oxygen abundance distribution in FGK dwarfs representative of the thin and thick disk Galactic populations.

2. Abundances in young open clusters and stellar associations

Open clusters (OCs) provide us with the best example in nature of a simple stellar population, that is an ensemble of coeval and (initially) chemically homogeneous group of stars. They have been largely used to probe different issues related to stellar and galactic evolution, including (but not limited to) radial and vertical gradients. OCs bring the strong advantage in that they span a wide range in metallicity (roughly a factor of ten, from sub-solar to super-solar $[\text{Fe}/\text{H}]$), age (from a few Myrs up to several Gyrs), and Galactocentric distance (see the seminal review by Friel et al. 2002 and references therein). The last decade witnessed a revolution in the chemical characterisation of stellar populations (including OCs) thanks to the large spectroscopic surveys (e.g., the Gaia-ESO Magrini et al. (2017), GALAH Spina et al. (2021); OCCAM Donor et al. (2020) and OCCASO Casamiquela et al. (2019)). Interestingly enough, the chemical composition of young clusters and stellar associations (ages $\lesssim 0.5 - 1$ Gyr) have been mostly overlooked, with a few exceptions. These systems present two striking anomalies: (i) there are no young metal-rich clusters in the solar neighbourhood, being all OCs with ages less than 200 Myr actually sub-solar; (ii) young OCs exhibit an extreme barium enhancement (up to ~ 0.6 dex level), which is not fol-

lowed by a similar trend in other s-process element abundances (expected especially for elements produced by the same peak of the s process, e.g., lanthanum, cerium). Both issues have been extensively investigated in our recent papers (Baratella et al. 2020b,a, 2021), to which we refer the reader for detailed discussions. Our main findings indicate that the peculiar behaviour shown by young OCs reflects errors in the chemical analysis of young stars. In particular, over-estimation of the microturbulence velocity parameters (V_t or ξ , as routinely labelled) results in both artificially low metallicity and high Ba abundances. As a preliminary solution we suggested the use of neutral and singly-ionised titanium lines to derive atmospheric parameters, because they are less sensitive to the magnetic activity (they form deeper in the stellar photosphere than iron lines, on average). Our revised metallicity for young open clusters (see Fig. 1) provides a good agreement with the Galactic chemical evolution model and suggests that young systems in the solar neighbourhood do not display a sub-solar metal content. As a consequence, we do not need to call for peculiar chemical evolution. We also suggest that the apparent flattening of the radial gradient at young ages (less than 1 Gyr), as revealed from OCs, might be related to the same effect of magnetic activity. Further investigation is sorely needed. In addition, we promote the use of lanthanum (instead of Ba) to trace the Galactic chemical evolution of the s process at young ages. Future work will be carried out towards manifold directions, most crucially by including the effect of magnetic fields in synthetic stellar spectra (Nordlander et al. 2022, in preparation).

3. Abundance gradients in the Milky Way from Cepheids

Recent determinations of the radial and azimuthal gradients using Cepheids yield slopes of ≈ -0.50 dex/kpc for the $[\text{Fe}/\text{H}]$ gradient, ≈ -0.45 dex/kpc for the α -elements, and of ≈ -0.025 dex/kpc for the neutron-capture elements (e.g., Lemasle et al. 2013; Genovali et al. 2013, 2014, 2015; da Silva et al. 2016; Luck 2018; Kovtyukh et al. 2022). There are little

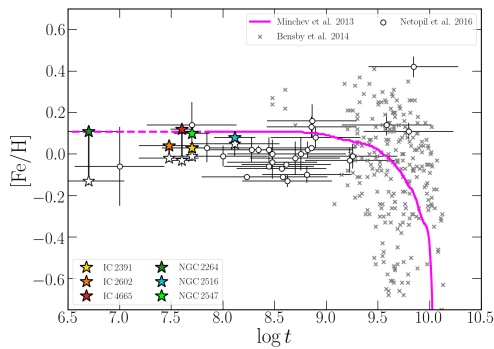


Fig. 1. Metallicity as a function of the age for six open clusters published in Baratella et al. (2020b). Field stars by (Bensby et al. 2014) along with the cluster compilation by (Netopil et al. 2016) are also shown. The Figure has been readapted from Baratella et al. (2020b)

uncertainties on distances - usually not taken into account for computing radial gradients (to our knowledge, only in Lemasle et al. 2018). However, there is still room for improvement regarding the determination of abundances.

3.1. Improving abundances in Cepheids

Since they are pulsating, no simultaneous photometry is usually available for determining the atmospheric parameters of Cepheids. All the information must be extracted from spectra, namely via line depth ratios (LDR) of carefully selected lines, calibrated against T_{eff} beforehand (see Proxauf et al. 2018, for the latest calibration). Although an excellent relative scale (~ 30 K), concerns have been raised regarding its accuracy (~ 150 K), probably degrading for long-period Cepheids ($P > 10$ d) or at phases of extreme compression of the atmosphere.

A first method to tackle this problem is provided by da Silva et al. (2022). Using 20 calibrating Cepheids with a large number of high signal-to-noise (S/N) spectra covering the entire pulsation period, they selected only lines with recent, accurate laboratory measurements for the atomic transition parameters. They discarded saturated and blended lines, lines with a poor definition of the continuum, lines pre-

sented systematic over- or under-abundance (presumably from inaccurate atomic data), and lines whose residual abundance with respect to the mean value correlates with T_{eff} , potentially indicative of NLTE effects. Light and radial velocity curves were phased using the epoch of the mean magnitude on the rising branch of the light curve, $T_{\text{mean}}^{\text{opt}}$ or, equivalently, the epoch of mean velocity on the decreasing branch of the radial velocity curve, $T_{\text{mean}}^{\text{RV}}$ (Inno et al. 2015; Braga et al. 2021).

Combining LDRs and a canonical spectroscopic analysis, they fitted Fourier series to the T_{eff} , $\log g$, and v_t curves for different period bins, improving their amplitudes by a factor > 2 thanks to the improved atmospheric parameters and the better sampling of the pulsation cycle (see Fig. 2). With these templates, one can derive $\langle T_{\text{eff}} \rangle$ from a single measurement and ephemerides.

Such a method facilitates the analysis of near-infrared spectra, which can be hampered by the modest number of (especially) ionized iron lines available. It opens the way for testing quantitatively nonlinear, convective hydrodynamical models of Cepheids (e.g., Marconi et al. 2013) and constraining the efficiency of the convective transport over the entire pulsation cycle.

Another technique was developed by Lemasle et al. (2020), who labelled in T_{eff} a similarly large (1324) sample of spectra for 24 calibrating Cepheids using the near-infrared surface-brightness (IRSB) method (Fouque & Gieren 1997), calibrated thanks to interferometric angular diameters of Cepheids (Kervella et al. 2004). The reddening toward the calibrating Cepheids is the only significant systematic uncertainty on the labels. They used a data-driven approach using flux ratios (FRs), developed by Hanke et al. (2018) for stable stars (ATHOS: A Tool for HOMogenizing Stellar parameters), to predict T_{eff} . Each component of the ratio is the mean flux of 5 pixels.

The training spectra are rebinned to a common resolution ($R=5000$), which limits the number of available relations but makes the training insensitive to photon noise as the already high S/N of the training spectra is further increased. Moreover, in the perspective

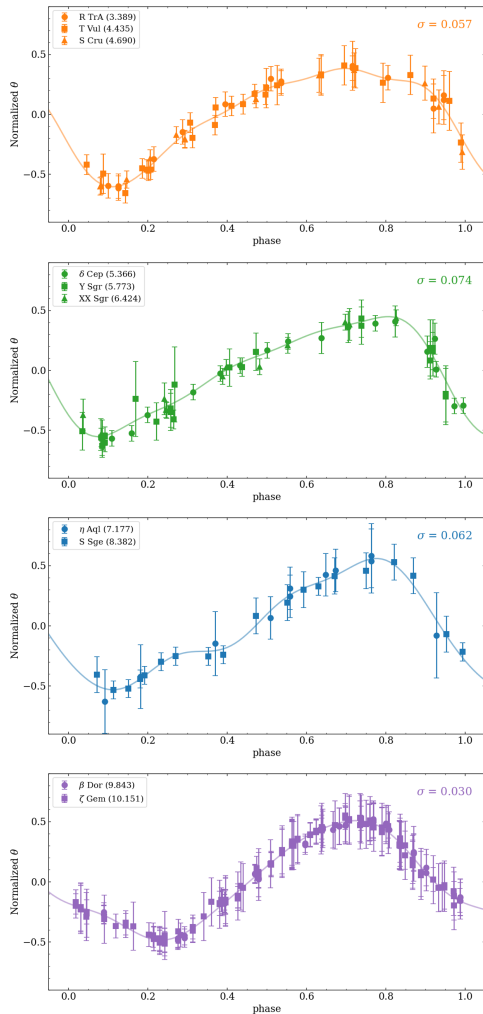


Fig. 2. Normalized Θ ($5040/T_{\text{eff}}$) as a function of the pulsation phase. The panels display phase-folded curves for different bins of pulsation period. The fits of the Fourier series to the data are over-plotted and the standard deviations of the fits are provided in the top-right.

of large spectroscopic surveys, it ensures that that low- and high-resolution spectra fall on the same T_{eff} scale. However, the lower resolution increases the sensitivity to metallicity via blending features, thus reducing the applicability of the method to the range of parameters (especially $[\text{Fe}/\text{H}]$) within the train-

ing sample. This is anyway mandatory with machine-learning techniques. Since it is also required that two flux domains remain within 30 pixels (further limiting the amount of relations), the continuum can be considered constant and the method does not require a continuum normalization. Selecting the FRs yielding precision/accuracy >3 and precision better than 100 K from all FRs whose Pearson linear correlation with the T_{eff} labels is >0.93 , Lemasle et al. (2020) obtained 143 calibration relations. Combined, they reproduce almost exactly the input T_{eff} scale, with an internal precision of a few K and an accuracy mostly lying within ± 10 K. Considering the test spectra altogether, small-scale residuals, partially phase-dependent, limit the overall accuracy to a few tens of K, nevertheless better than any current alternative method.

3.2. Cepheids trace the spiral arms

Using mid-infrared photometry and an updated catalog of Galactic Cepheids, Lemasle et al. (2022) used a clustering algorithm to identify groups of Cepheids in the $(\theta, \ln r)$ space. θ and r are the Galactocentric longitude and distance (corrected from the effects of the warp) of individual Cepheids. The sample is limited to Cepheids younger than 150 Myr, with ages derived from the period-age relations provided by Bono et al. (2005). Cepheids groups trace portions of spiral arms in the (θ, r) space, even at large distances from the Sun (Fig.3). This could be achieved so far only thanks to masers (Reid et al. 2019), which have the advantage that their very young age ensures that they had no time to evolve off their birthplace, but are far less numerous than Cepheids.

4. Giants In the Local Disk: Abundances of about 30 elements from high-resolution spectra of about 500 stars

We live in the era of stellar spectroscopic surveys, greatly extending the number of spectroscopically characterized stars, also to stellar populations not so well studied previously. Examples of such survey projects in-

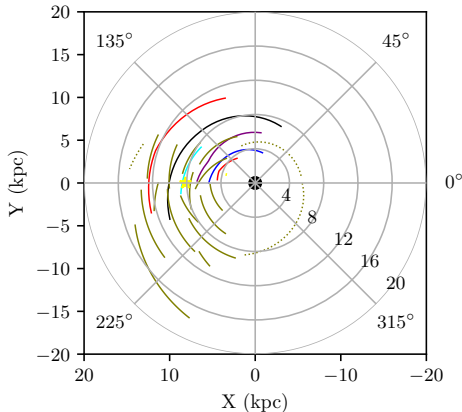


Fig. 3. Spiral segments (olive) over-plotted on the spiral arms model of Reid et al. (2019), the spiral arms are displayed using the same color-coding as in the original paper (Red: Norma-Outer, blue: Sct-Cen, purple: Sgr-Car, cyan: Local, black: Perseus).

clude Gaia-ESO (Gilmore et al. 2012; Randich et al. 2013), APOGEE (Majewski et al. 2017), GALAH (De Silva et al. 2015), and more. These enormous databases can be used to address a plethora of science questions, for example within the field often referred to as Galactic archaeology. Within those projects, the spectral analysis is by necessity made on an industrial scale and the amount of manual interventions, traditionally customary in the analysis of stellar spectra, is forced to be minimal. Instead, the result of the industrial pipeline is often evaluated by comparing the results to previous small-scale, high-precision, “by-hand” analyses of much smaller samples of stars (see for example Jönsson et al. 2018, 2020). Ideally, these samples should be made up of stars in the “known” stellar population of the local disk, and have as many different elemental abundances as possible determined for a wide spread of metallicities. Such “trusted” samples of nearby disk stars are available for dwarf stars with for example the series of papers starting with Bensby et al. (2014) or Adibekyan et al. (2012), while not many of the

same type of high-precision samples of disk giants exist. This is of course not surprising; why go through the hassle of analyzing giant stars when investigating the solar neighborhood where high S/N-spectra of the more easily analyzed dwarf stars can be recorded using rather short integration times on moderate-sized telescopes? The need for these kinds of giant stars samples has not arisen until now, with evaluation of the spectroscopic surveys. The giant stars of the surveys are often among the most interesting stars, since these tend to be the most distant, and hence the evaluation of the performance of the spectroscopic survey analysis pipelines for the giant stars is important.

This need is where the project Giants In the Local Disk (GILD) takes its start: by simply providing high-precision stellar parameters and abundances for as many elements as possible in a mid-sized sample of stars, with the aim of providing a way of assessing the performance of more automatic stellar spectroscopy analysis pipelines.

Data for the project has been collected from five observational runs (25 nights in total) using the spectrometer FIES on the Nordical Optical Telescope (NOT) on La Palma. In addition, several searches for known giant star spectra have been made in the FIES-archive over the years. In total 598 spectra of 579 stars have been collected. FIES has a resolving power of $R \sim 67000$, and the usable wavelength-range in these giant star spectra is 4100-7359 Å. Some statistics of the sample is shown in Figure 4.

The analysis of the spectra is made using the code PySME¹, which is a python-translated version of the widely used SME-code (Valenti & Piskunov 1996; Piskunov & Valenti 2017). PySME/SME fits the user’s pre-defined parts of a synthetic spectrum to the observed spectrum, varying whatever free parameter(s) specified. In this way, masks covering Fe I, Fe II, and Mg I lines are used to simultaneously adjust and hence determine the T_{eff} , $\log g$, $[\text{Fe}/\text{H}]$, v_{mic} , v_{mac} , v_{rad} , and $[\text{Mg}/\text{Fe}]$ in the stars. After this, elemental abundances are determined us-

¹ <https://github.com/AWehrhahn/SME>

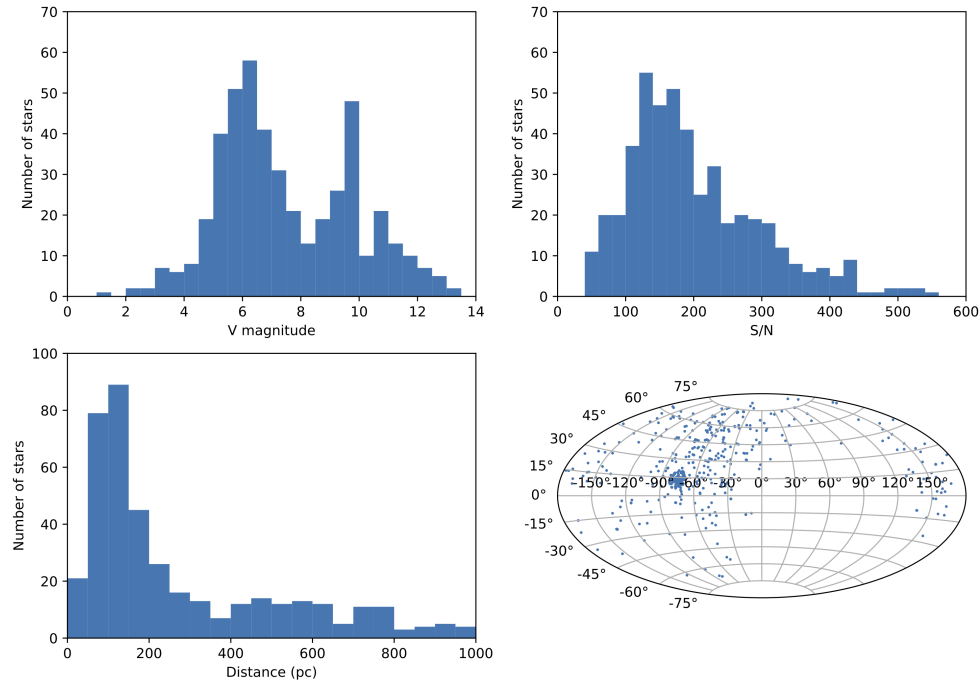


Fig. 4. Some statistics of the GILD-sample of giant stars, and the spectra recorded.

ing well-chosen suits of lines for every element of interest. During this process, every fit of every line in every spectrum is manually inspected to ensure high quality in the final results.

As this is a work in progress (H. Jönsson, R. Forsberg, et al. in prep.), not all the planned abundances have been determined; so far abundances of C, N, O, Na, Mg, Al, Si, Ca, Sc, Ti, V, Cr, Mn, Fe, Co, Ni, Cu, Y, Zr, Mo, La, Ce, Pr, Nd, Eu, and Gd are finished, and Li, S, K, Zn, Sr, Nb, Ru, Ba, Sm are on the list on what to try next. This means that the number of different elemental abundances might be over 30, and will cover most of the elements investigated in the modern spectroscopic surveys.

Future plans within this project include a second iteration of the same type of analysis, but instead using archive data from the ESPaDOnS spectrometer on the Canadian French Hawaiian Telescope (CFHT), thereby extending the sample to even more stars. ESPaDOnS has about the same resolving power as FIES ($R \sim 65000$ or $R \sim 80000$

depending on setting) but goes higher in the red (up to 10465\AA), possibly providing lines for new elements to be determined in these spectra, in addition to the 30-ish abundances listed above for the FIES-spectra (S. Bijavara Seshashayana, H. Jönsson et al. in prep.).

5. Oxygen in the Galactic disks

Oxygen is the third most abundant element in the Universe. The analysis of elemental abundances in the atmospheres of long-lived FGK dwarf stars allows to determine the chemical composition of the gas from which the stars were originated but also to trace the chemical history in the different stellar populations in the Milky Way. In this respect the oxygen fossil is often used in models of Galactic evolution. Unfortunately, the atomic lines suitable to derive the O abundance are not numerous in the visual spectrum of these stars, and all of them present some difficult issues and produce also discordant results according to the different lines (e.g., Bertran de Lis et al. 2015).

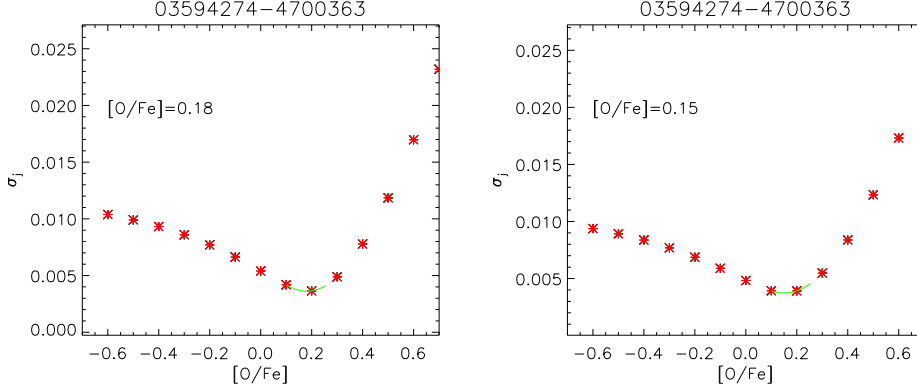


Fig. 5. Example of $[O/Fe]$ measurement for a GES star. Trends of σ_j vs. $[O/Fe]$ (red dots) and parabolic interpolations (green lines) when the standard deviations (σ_j) are computed in the region $\lambda_0 \pm \Delta\lambda_{\text{rot}}$ where $\lambda_0 = 6300.3 \text{ \AA}$, $\Delta\lambda_{\text{rot}} = (v \sin i + \epsilon_{v \sin i})\lambda_0/c$ (left panel) and only half profile, i.e. the blue wing $\lambda_0 - \Delta\lambda_{\text{rot}}$ (right panel). The “best” $[O/Fe]$ value corresponds to the position of the minimum in the parabolic fitting.

Therefore, the distribution of $[O/Fe]$ in stars across the Galactic disk(s) is still under debate.

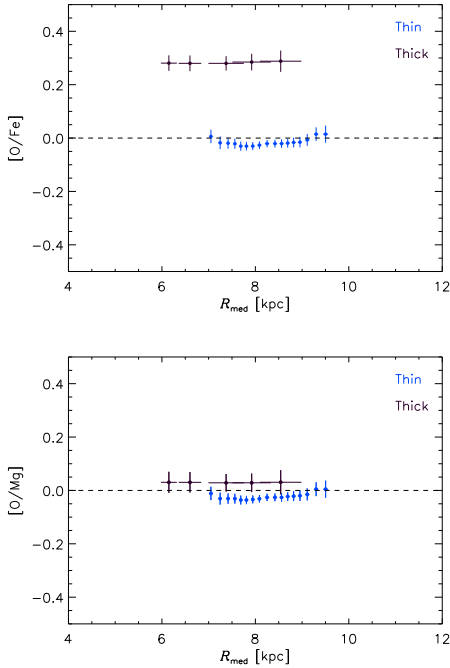


Fig. 6. $[O/Fe]$ (top) and $[O/Mg]$ (bottom panel) versus R_{med} for thin and thick disk star samples.

Many efforts have been made in recent years to understand the discrepancies derived by the different lines adopted to estimate oxygen abundance and their effect on the analysis of oxygen trends in the disk populations of our Galaxy (e.g., Bertran de Lis et al. 2015). In addition to all of these numerous and accurate works, the large modern spectroscopic surveys, such as the Gaia-ESO spectroscopic Survey (GES, Gilmore et al. 2012; Randich et al. 2013), the Apache Point Observatory Galactic Evolution Experiment (APOGEE, Majewski et al. 2017), and GALactic Archaeology with HERMES (GALAH, De Silva et al. 2015), have provided statistically significant samples of FGK stars. The studies of the chemical properties of the Galactic stellar populations from the above-quoted surveys have still provided discrepant results. For example, Weinberg et al. (2019) derived the median trends of abundance ratios $[O/Mg]$ versus $[Mg/H]$ from more than 20,000 stars within the SDSS-APOGEE survey and found that $[O/Mg]$ barely correlates with $[Mg/H]$. Conversely, Griffith et al. (2019) from their large GALAH sample found a strong correlation with $[O/Mg]$ values that significantly decrease with increasing $[Mg/H]$.

In order to contribute to our understanding of the evolution of oxygen, we take advantage of UVES spectra in the fifth GES internal data

release (iDR5) to derive oxygen abundances for a sample of more than 500 FGK dwarf stars belonging to the Galactic thin and thick disks. These stars are a sub-sample of 2133 stars whose carbon abundances were derived from atomic lines in Franchini et al. (2020, hereafter FR20) where more details about our observational data-set can be found. We used the [O I] 6300.3 Å forbidden line, which is unaffected by NLTE effects. In particular, we adopted a spectral synthesis technique. For each star, we computed 13 atmosphere models with the GES iDR5 atmospheric parameter values (effective temperature, surface gravity, iron abundance, micro-turbulence) and individual element abundances with the only exception of [C/Fe] values which are from FR20, and differing only in [O/Fe], i.e., with $[O/Fe]_j = -0.6 + (j-1) \cdot 0.1$ dex (with $j=1, \dots, 13$). We used the stellar atmosphere ATLAS12 code (Kurucz 2005) to compute a model atmosphere and the spectral synthesis program SPECTRUM v2.76f (Gray & Corbally 1994) to compute the corresponding synthetic spectrum. The synthetic spectra were used to normalize the observed one in the region of the 6300 line as described in FR20 and Franchini et al. (2021, hereafter FR21).

For each star we computed the standard deviation (σ_j) between the observed spectrum and the 13 synthetic spectra with the different [O/Fe] values in a spectral range centered at 6300.3 Å and with a width proportional to the stellar rotational velocity, $v \sin i$, taking into account also its uncertainty, $\epsilon_{v \sin i}$, (Fig. 5 left panel). Moreover, the same fitting procedure was applied to only half of the [O I] profile, i.e., the blue wing (5 wright panel), to avoid any systematic error due to the use of a possible incorrect Ni abundance in considering the blend effect of the Ni lines that is much stronger in the red part of the [O I] profile. Only stars/spectra with a standard deviation of the two obtained [O/Fe] values lower than $3\sigma_{[O/Fe]}$ were accepted and we obtained trustworthy [O/Fe] abundance ratios for 516 dwarfs.

The analysis of the derived O abundances was done for two sub-samples representative of the thin and thick discs with the aim of investigating possible differences in their O content and of understanding the origin of the

Galactic oxygen enrichment. The Galactic thin and thick disks are two distinct stellar populations in terms of age distributions, chemistry, and kinematics. The two samples representative of local thin and thick disks was defined using three different selection methodologies: the chemical method (i.e. the [Mg/Fe]-[Fe/H] plane), the kinematical method based on stellar Galactic velocities, and the orbital parameters of the stars (see FR20 and FR21). Among the many interesting results that emerged from the analysis of our measured O abundances (FR21), it is worthwhile mentioning here the systematic difference between the [O/Fe] content in the thin and thick disc populations at a given [Fe/H], with the thick disc being more enhanced in [O/Fe] and [O/H] with respect to thin disc stars. Our result suggests that the oxygen enrichment is mostly due to massive stars, through core-collapse supernovae, with no evidence of contributions from SNIa or AGB stars. Moreover, we found that O and Mg do not evolve in lockstep and thus they might have a different origin with Mg that might also be partially released into the interstellar medium by SNIa (see also Magrini et al. 2017). As far as Mg is concerned, here we only show in Fig. 6 the radial gradient of [O/Fe] and [O/Mg] versus galactocentric distances R_{med} (the mean of the apo- and pericentersiniric distances of the stellar orbit) for the thin and thick disk stars, using a running average. We observe a flat (or slightly positive trend for the thin disk star bins. The large [O/Fe] difference between thin and thick disk is notoriously due to the longer timescale for Fe enrichment by SNeI, while the small difference in [O/Mg] suggests that O and Mg are produced by stars with similar lifetimes (hence similar masses), although not equal. Since there seems to be more Mg in the thin than in the thick disk, this suggests that the producers of Mg have slightly longer lifetimes than O producers.

Acknowledgements. BL acknowledges the Deutsche Forschungsgemeinschaft (DFG, German Research Foundation) – Project-ID 138713538 – SFB 881 (“The Milky Way system”, sub-projects A05).

References

- Adibekyan, V. Z., Sousa, S. G., Santos, N. C., et al. 2012, *A&A*, 545, A32
- Baratella, M., D’Orazi, V., Biazzo, K., et al. 2020a, *A&A*, 640, A123
- Baratella, M., D’Orazi, V., Carraro, G., et al. 2020b, *A&A*, 634, A34
- Baratella, M., D’Orazi, V., Sheminova, V., et al. 2021, *A&A*, 653, A67
- Bensby, T., Feltzing, S., & Oey, M. S. 2014, *A&A*, 562, A71
- Bertran de Lis, S., Delgado Mena, E., Adibekyan, V. Z., Santos, N. C., & Sousa, S. G. 2015, *A&A*, 576, A89
- Bono, G., Marconi, M., Cassisi, S., et al. 2005, *ApJ*, 621, 966
- Braga, V. F., Crestani, J., Fabrizio, M., et al. 2021, *ApJ*, 919, 85
- Casamiquela, L., Blanco-Cuaresma, S., Carrera, R., et al. 2019, *MNRAS*, 490, 1821
- Costa, R. D. D., Uchida, M. M. M., & Maciel, W. J. 2004, *A&A*, 423, 199
- da Silva, R., Crestani, J., Bono, G., et al. 2022, arXiv e-prints, arXiv:2202.07945
- da Silva, R., Lemasle, B., Bono, G., et al. 2016, *A&A*, 586, A125
- Daflon, S. & Cunha, K. 2004, *ApJ*, 617, 1115
- De Silva, G. M., Freeman, K. C., Bland-Hawthorn, J., et al. 2015, *MNRAS*, 449, 2604
- Donor, J., Frinchaboy, P. M., Cunha, K., et al. 2020, *AJ*, 159, 199
- Fouque, P. & Gieren, W. P. 1997, *A&A*, 320, 799
- Franchini, M., Morossi, C., Di Marcantonio, P., et al. 2021, *AJ*, 161, 9
- Franchini, M., Morossi, C., Di Marcantonio, P., et al. 2020, *ApJ*, 888, 55
- Friel, E. D., Janes, K. A., Tavaréz, M., et al. 2002, *AJ*, 124, 2693
- Gaia Collaboration et al. 2016, arXiv preprint arXiv:1609.04153
- Genovali, K., Lemasle, B., Bono, G., et al. 2014, *A&A*, 566, A37
- Genovali, K., Lemasle, B., Bono, G., et al. 2013, *A&A*, 554, A132
- Genovali, K., Lemasle, B., da Silva, R., et al. 2015, *A&A*, 580, A17
- Gilmore, G., Randich, S., Asplund, M., et al. 2012, *The Messenger*, 147, 25
- Gray, R. O. & Corbally, C. J. 1994, *AJ*, 107, 742
- Griffith, E., Johnson, J. A., & Weinberg, D. H. 2019, *ApJ*, 886, 84
- Hanke, M., Hansen, C. J., Koch, A., & Grebel, E. K. 2018, *A&A*, 619, A134
- Harris, H. C. 1981, *AJ*, 86, 707
- Inno, L., Matsunaga, N., Romaniello, M., et al. 2015, *A&A*, 576, A30
- Jönsson, H., Allende Prieto, C., Holtzman, J. A., et al. 2018, *AJ*, 156, 126
- Jönsson, H., Holtzman, J. A., Allende Prieto, C., et al. 2020, *AJ*, 160, 120
- Kervella, P., Bersier, D., Mourard, D., et al. 2004, *A&A*, 428, 587
- Kovtyukh, V., Lemasle, B., Bono, G., et al. 2022, *MNRAS*, 510, 1894
- Kurucz, R. L. 2005, *Memorie della Societa Astronomica Italiana Supplementi*, 8, 14
- Lemasle, B., François, P., Genovali, K., et al. 2013, *A&A*, 558, A31
- Lemasle, B., Hajdu, G., Kovtyukh, V., et al. 2018, *A&A*, 618, A160
- Lemasle, B., Hanke, M., Storm, J., Bono, G., & Grebel, E. K. 2020, *A&A*, 641, A71
- Lemasle, B., Lala, H. N., Kovtyukh, V., et al. 2022, arXiv e-prints, arXiv:2209.02731
- Luck, R. E. 2018, *AJ*, 156, 171
- Magrini, L., Randich, S., Kordopatis, G., et al. 2017, *A&A*, 603, A2
- Majewski, S. R., Schiavon, R. P., Frinchaboy, P. M., et al. 2017, *AJ*, 154, 94
- Marconi, M., Molinaro, R., Bono, G., et al. 2013, *ApJ*, 768, L6
- Matteucci, F. & Francois, P. 1989, *MNRAS*, 239, 885
- Netopil, M., Paunzen, E., Heiter, U., & Soubiran, C. 2016, *A&A*, 585, A150
- Piskunov, N. & Valenti, J. A. 2017, *Astronomy & Astrophysics*, 597, A16
- Proxauf, B., da Silva, R., Kovtyukh, V. V., et al. 2018, *A&A*, 616, A82
- Randich, S., Gilmore, G., & Gaia-ESO Consortium. 2013, *The Messenger*, 154, 47
- Reid, M. J., Menten, K. M., Brunthaler, A., et al. 2019, *ApJ*, 885, 131
- Spina, L., Ting, Y. S., De Silva, G. M., et al. 2021, *MNRAS*, 503, 3279
- Tosi, M. 1996, in *Astronomical Society of*

- the Pacific Conference Series, Vol. 98, From Stars to Galaxies: the Impact of Stellar Physics on Galaxy Evolution, ed. C. Leitherer, U. Fritze-von-Alvensleben, & J. Huchra, 299
- Vilchez, J. M. & Esteban, C. 1996, MNRAS, 280, 720
- Weinberg, D. H., Holtzman, J. A., Hasselquist, S., et al. 2019, ApJ, 874, 102
- Valenti, J. A. & Piskunov, N. 1996, Astronomy and Astrophysics Supplement, 118, 595